

Up-regulation of the Fidelity of Human DNA Polymerase λ by Its Non-enzymatic Proline-rich Domain*

Received for publication, February 7, 2006, and in revised form, May 1, 2006. Published, JBC Papers in Press, May 4, 2006, DOI 10.1074/jbc.M601178200

Kevin A. Fiala^{†§1}, Wade W. Duym[‡], Jun Zhang[‡], and Zucai Suo^{†§¶**2}

From the [†]Department of Biochemistry, the [‡]Biochemistry Program, the [¶]Biophysics Program, the ^{||}Molecular, Cellular & Developmental Biology Program, and the ^{**}Comprehensive Cancer Center, The Ohio State University, Columbus, Ohio 43210

DNA repair pathways are essential for maintaining genome stability. DNA polymerase β plays a critical role in base-excision repair *in vivo*. DNA polymerase λ , a recently identified X-family homolog of DNA polymerase β , is hypothesized to be a second polymerase involved in base-excision repair. The full-length DNA polymerase λ is comprised of three domains: a C-terminal DNA polymerase β -like domain, an N-terminal BRCA1 C-terminal domain, and a previously uncharacterized proline-rich domain. Strikingly, pre-steady-state kinetic analyses reveal that, although human DNA polymerase λ has almost identical fidelity to human DNA polymerase β , the C-terminal DNA polymerase β -like domain alone displays a dramatic, up to 100-fold loss in fidelity. We further demonstrate that the non-enzymatic proline-rich domain confers the increase in fidelity of DNA polymerase λ by significantly lowering incorporation rate constants of incorrect nucleotides. Our studies illustrate a novel mechanism, in which the DNA polymerase fidelity is controlled not by an accessory protein or a proofreading exonuclease domain but by an internal regulatory domain.

A growing number of polymerases have been identified recently and many are hypothesized to function in DNA repair pathways. One of these polymerases is DNA polymerase λ ($\text{pol}\lambda$),³ a new member of the X-family DNA polymerases (1–3). This family of DNA polymerases is a subdivision of a larger superfamily of nucleotidyltransferases (4). Human DNA polymerase λ is encoded by a gene located in human chromosome 10 (2, 3). The N terminus of the full-length $\text{pol}\lambda$ ($\text{fpol}\lambda$) is composed of a nuclear localization signal motif, a breast cancer susceptibility protein BRCA1 C-terminal (BRCT) domain, and a proline-rich domain (see Fig. 1). BRCT domains are known to mediate protein-protein and protein-DNA interactions in

DNA repair mechanisms and cell-cycle checkpoint regulation upon DNA damage (5). The proline-rich domain, which contains multiple serine, threonine, and proline residues, is found to functionally suppress the polymerase activity of $\text{pol}\lambda$ (6) and limit strand-displacement synthesis (7). The C terminus of $\text{pol}\lambda$ ($\text{tPol}\lambda$ in Fig. 1) possesses both 5'-deoxyribose-5-phosphate lyase and DNA polymerase activities while sharing 33% sequence identity with DNA polymerase β ($\text{pol}\beta$) (1–3, 8). $\text{pol}\beta$, on the other hand, is also an X-family polymerase and is known to be involved in base excision repair (BER) pathways *in vivo* (9, 10). The x-ray crystal structures of $\text{tpol}\lambda$ (11, 12) display a high degree of similarity with the corresponding subdomains of $\text{pol}\beta$ (13, 14), including the deoxyribose-5-phosphate lyase (also known as the 8-kDa domain), fingers, palm, and thumb subdomains. A comparison of the crystal structures of $\text{tpol}\lambda$ -single-nucleotide gapped DNA, $\text{tpol}\lambda$ -single-nucleotide gapped DNA-ddTTP, and $\text{tpol}\lambda$ -nicked DNA-pyrophosphate suggests that no major protein domain movement occurs during catalysis (11). $\text{pol}\lambda$, like $\text{pol}\beta$, lacks 3'→5' exonuclease activity (1–3) and possesses low processivity when copying non-gapped DNA (8).

At present, the biological role of $\text{pol}\lambda$ is unknown. $\text{pol}\lambda$ has been suggested to play a role in DNA repair synthesis associated with meiosis (1), in "short-patch" BER (15, 16), in the proliferating cell nuclear antigen-dependent BER pathway (15, 17), and in the repair of double-stranded breaks through non-homologous end-joining pathways (15, 18, 19). All these potential physiological functions require $\text{pol}\lambda$ to possess gap-filling polymerase activity. The fidelity of $\text{pol}\lambda$ when filling medium to large gaps has been estimated to be in the range of 10^{-4} by both forward and reverse mutation assays (8, 17, 18). But the fidelity of the full-length $\text{pol}\lambda$ when filling single-nucleotide-gapped DNA, which is relevant to BER, has not been determined. Previously, we measured the base substitution fidelity for filling single-nucleotide-gapped DNA catalyzed by human $\text{tpol}\lambda$ and found it to be in the range of 10^{-2} – 10^{-4} , which is relatively low when compared with $\text{pol}\beta$ (15). However, the presence of the N-terminal BRCT and proline-rich domains may have significant effects on the fidelity of $\text{pol}\lambda$. Here, we use pre-steady-state kinetic methods to determine the base substitution fidelity of human $\text{fpol}\lambda$ and its N-terminal domain truncation fragments (see Fig. 1), based on all possible dNTP incorporations into single-nucleotide gapped DNA. Any difference in the fidelity between the full-length and the truncated $\text{pol}\lambda$ fragments will reveal the role of the BRCT and proline-rich

* This work was supported in part by a startup fund (to Z. S.) provided by the Ohio State University. The costs of publication of this article were defrayed in part by the payment of page charges. This article must therefore be hereby marked "advertisement" in accordance with 18 U.S.C. Section 1734 solely to indicate this fact.

¹ Supported by the National Institutes of Health Chemistry and Biology Interface Program at the Ohio State University (Grant T32 GM08512-08) and the American Heart Association Predoctoral Fellowship (Grant 0415129B).

² To whom correspondence should be addressed: 740 Biological Sciences, 484 West 12th Ave., Columbus, OH 43210. Tel.: 614-688-3706; Fax: 614-292-6773; E-mail: suo.3@osu.edu.

³ The abbreviations used are: $\text{pol}\lambda$, DNA polymerase λ ; $\text{pol}\beta$, DNA polymerase β ; BER, base excision repair; BRCT, breast cancer susceptibility gene 1 C-terminal domain; $\text{fpol}\lambda$, full-length $\text{pol}\lambda$; $\text{dpol}\lambda$, $\text{pol}\lambda$ fragment (residues 132–575); $\text{tpol}\lambda$, $\text{pol}\lambda$ fragment (residues 245–575); DTT, dithiothreitol.

domains in polymerization efficiency and fidelity. Our kinetic results strongly support a role for pol λ as the second polymerase in BER.

MATERIALS AND METHODS

Cloning, Expression, and Purification of fpol λ , dpol λ , and tpol λ —Preparation of tpol λ fused to a C-terminal His $_6$ tag (38.2 kDa) was described previously (15). The human genes encoding fpol λ and dpol λ (Fig. 1) were PCR-amplified and separately inserted into the NdeI/XhoI sites of pET28b and pET24b to construct pET28b-fpol λ and pET24b-dpol λ . A stop codon was engineered before the XhoI site of pET28b-fpol λ . The constructed plasmids were individually transformed into *Escherichia coli* strain BL21 CodonPlus (DE3)-RIL competent cells (Stratagene) to express fpol λ fused to both an N-terminal and a C-terminal hexahistidine tag, and dpol λ fused to a C-terminal hexahistidine tag. Both fpol λ (65.6 kDa) and dpol λ (50.1 kDa) were overexpressed in these transformed *E. coli* cells as was tpol λ (15). fpol λ was purified through a nickel-nitrilotriacetic acid column (Qiagen), a heparin-Sepharose Fast Flow column (GE Healthcare), a DEAE-Sepharose column (GE Healthcare), and a Mono-S 10/10 column (GE Healthcare). dpol λ was purified through a nickel-nitrilotriacetic acid column (Qiagen), a heparin-Sepharose Fast Flow column, a DEAE-Sepharose column, and a HiTrap Q column (GE Healthcare). The His $_6$ tags of purified fpol λ and dpol λ were detected by Western blot analysis using anti-hexahistidine tag antibody (data not shown). The concentrations of the purified fpol λ and dpol λ were measured spectrophotometrically at 280 nm using the calculated extinction coefficients of 61,615 and 48,204 M $^{-1}$ cm $^{-1}$, respectively.

Synthetic Oligodeoxyribonucleotides—The oligodeoxyribonucleotides in Fig. 2 were purchased from Integrated DNA Technologies and purified by denaturing polyacrylamide gel electrophoresis (18% acrylamide, 8 M urea). Their concentra-

tions were determined by UV absorbance at 260 nm with calculated extinction coefficients. The 21-mer was 5'-end-labeled by using Optikinase (U. S. Biochemical Corp.) and [γ - 32 P]ATP (PerkinElmer Life Sciences), and subsequently purified using a Biospin column (Bio-Rad Laboratories). Each single-nucleotide-gapped DNA substrate was prepared by heating a mixture of 21-mer, 19-mer, and 41-mer in a 1:1.25:1.15 molar ratio, respectively, for 8 min at 95 °C, then cooling the mixture slowly to room temperature over 3 h as described previously (15).

Reaction Buffer L—Buffer L contains 50 mM Tris-Cl (pH 8.4 at 37 °C), 5 mM MgCl $_2$, 100 mM NaCl, and 0.1 mM EDTA, 5 mM DTT, 10% glycerol, and 0.1 mg/ml bovine serum albumin. Buffer L was the optimized buffer used previously for studies probing the fidelity and mechanism of human tpol λ (15). All reactions reported in this paper were carried out in buffer L and at 37 °C. All concentrations refer to concentrations of components after mixing.

Determination of the Equilibrium Dissociation Constant (K_d) and the Maximum Rate Constant of Nucleotide Incorporation (k_p) of an Incoming Nucleotide—Both k_p and K_d were determined by mixing a preincubated solution of full-length pol λ and DNA at fixed concentrations with increasing concentrations of an incoming nucleotide (Invitrogen) in buffer L at 37 °C. These reactions were quenched at various times via the addition of 0.37 M EDTA. For the fast incorporation of a correct nucleotide, the reactions were carried out using a rapid chemical quenched-flow apparatus (KinTek). Aliquots of the quenched reactions were analyzed by sequencing gel analysis (17% acrylamide, 8 M urea, 1 \times Tris borate- EDTA running buffer) and quantitated using a PhosphorImager 445 SI (Molecular Dynamics). The resulting time courses of product formation were fit to a single exponential equation (Equation 1) using the nonlinear regression program KaleidaGraph (Synergy Software) for each concentration of Mg $^{2+}$ -dNTP to give the observed rate constant of nucleotide incorporation (k_{obs}). The corresponding observed incorporation rate constants were plotted against the concentrations of Mg $^{2+}$ -dNTP, and these data were fit to a hyperbola (Equation 2) using KaleidaGraph to give K_d and k_p as follows.

$$[\text{Product}] = A[1 - \exp(-k_{obs}t)] \quad (\text{Eq. 1})$$

$$k_{obs} = k_p[\text{dNTP}]/\{[\text{dNTP}] + K_d\} \quad (\text{Eq. 2})$$

RESULTS

Fidelity of Full-length Human pol λ —Previously, we established a minimal kinetic mechanism (Scheme 1) for the single-nucleotide gap-filling activity of tpol λ (15). Scheme 1 shows that an incoming deoxyribonucleotide binds to the E-DNA binary complex to establish a rapid equilibrium prior to nucleotide incorporation. We expect the full-length pol λ to have similar polymerase activity as tpol λ and thus follow the same minimal mechanism shown in Scheme 1. This mechanism allows us to measure the apparent affinity of dNTP (K_d) for the

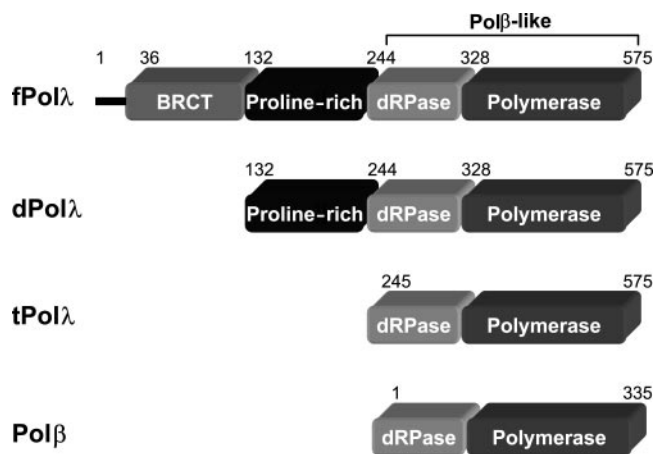
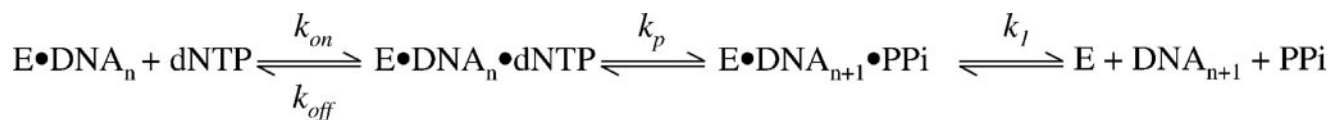


FIGURE 1. Schematic representations of human fpol λ , dpol λ , tpol λ , and pol β . Each domain, with amino acid residue numbers indicated above, is shown as a rectangle. The N-terminal 35 residues of fpol λ containing a nuclear localization signal motif are shown as the line.



SCHEME 1

Fidelity of DNA pol λ Measured by Transient Kinetics

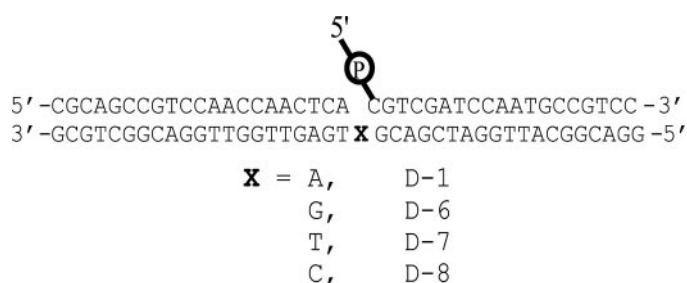


FIGURE 2. **Single-nucleotide-gapped DNA substrates D-1, D-6, D-7, and D-8.** Primer 21-mer was 5'- ^{32}P -labeled. The downstream primer 19-mer was 5'-phosphorylated (circled 'P'). "X" represents the unpaired base of template 41-mer.

fpol λ ·DNA binary complex via the dNTP concentration dependence of the observed single-turnover rate constant (k_{obs}). Our results shown below confirm this hypothesis. The single-turnover method was employed because DNA dissociates from tpol λ with a dissociation rate constant (k_1) that is ~ 2 - to 3-fold slower than the maximum nucleotide incorporation rate constant k_p (15), rendering the burst phase (amplitude = $[k_p/(k_p + k_1)]^2$) small. Thus, the experiments were performed with fpol λ in molar excess over DNA (or under single-turnover conditions) to avoid complication from the steady-state reaction phase (20). A preincubated solution of 5'- ^{32}P -labeled D-1 (Fig. 2) and 4-fold fpol λ was reacted with increasing concentrations of correct dTTP in buffer L. The DNA product 22-mer and remaining primer 21-mer at different time intervals were separated and quantitated. The product concentration was plotted against reaction time intervals. These data were subsequently fit to Equation 1, to yield a single-turnover rate constant at each concentration of dTTP (Fig. 3A). The single-turnover rates were then plotted against dTTP concentrations (Fig. 3B). These data were subsequently fit to Equation 2 (see "Materials and Methods"), to yield a k_p of $3.9 \pm 0.2 \text{ s}^{-1}$ for the maximum dTTP incorporation rate constant, and a K_d of $2.6 \pm 0.4 \mu\text{M}$ for dTTP binding. The substrate specificity (k_p/K_d) of dTTP incorporation into D-1 was calculated to be $1.5 \times 10^6 \text{ M}^{-1} \text{ s}^{-1}$ (Table 1).

Similar pre-steady-state kinetic analyses were used to determine the kinetic parameters (Table 1) for the incorporation of each of the remaining three correct nucleotides (dCTP into D-6, dATP into D-7, and dGTP into D-8), and for the incorporation of each of the 12 possible misincorporations into D-1, D-6, D-7, and D-8 (Fig. 2). Notably, the ground-state-binding affinity of all nucleotides to the fpol λ ·DNA (Table 1) and the tpol λ ·DNA (15) binary complexes were similar, but the maximum incorporation rate constants, particularly for incorrect nucleotides, with fpol λ (Table 1) were slower than the corresponding parameters for tpol λ measured previously (15). The substrate specificity (k_p/K_d) of all four correct nucleotides was slightly lower for fpol λ when compared with tpol λ (Fig. 4A) with a nucleotide incorporation efficiency ratio, $(k_p/K_d)_{\text{tpol}\lambda}/(k_p/K_d)_{\text{fpol}\lambda}$, less than 2 (Table 1). In contrast, fpol λ incorporated incorrect nucleotides with much lower substrate specificities than tpol λ (Table 1 and Fig. 4B). The nucleotide incorporation efficiency ratio, $(k_p/K_d)_{\text{tpol}\lambda}/(k_p/K_d)_{\text{fpol}\lambda}$, was calculated to be in the range of 10–100 for all twelve incorrect base pairs (Table 1). The variation in this ratio was due to the

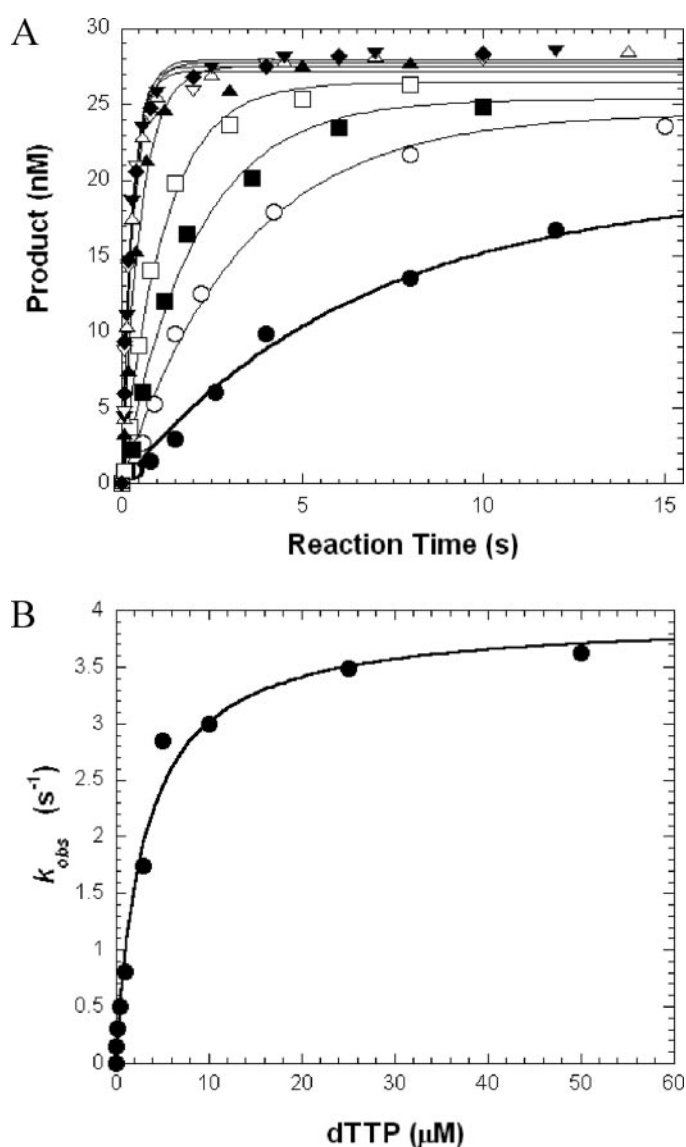


FIGURE 3. **dTTP incorporation into 5'- ^{32}P -labeled D-1.** Concentration dependence of the pre-steady-state rate of correct deoxyribonucleotide incorporation. **A**, a preincubated solution of pol λ (120 nM) and ^{32}P -labeled D-1 (30 nM) was rapidly mixed with increasing concentrations of Mg^{2+} -dTTP (\bullet , 0.1 μM ; \circ , 0.25 μM ; \blacksquare , 0.5 μM ; \square , 1 μM ; \blacktriangle , 3 μM ; \triangle , 5 μM ; \blacktriangledown , 10 μM ; \triangledown , 25 μM ; and \blacklozenge , 50 μM) for various time intervals. The *solid lines* are the best fits to the single exponential equation (Equation 1). **B**, the single exponential rates obtained from the above data fitting were plotted as a function of dTTP concentration. The extracted rate data were then fit to the hyperbolic equation (Equation 2) yielding a k_p of $3.9 \pm 0.2 \text{ s}^{-1}$ and a K_d of $2.6 \pm 0.4 \mu\text{M}$.

sequence dependence of polymerization catalyzed by DNA polymerases. Nevertheless, the large ratios suggest that fpol λ achieves significantly higher fidelity than tpol λ by lowering the incorporation efficiency of mismatched nucleotides. To confirm this possibility, we calculated the fidelity of fpol λ , which was sequence-dependent and in the range of 10^{-4} – 10^{-5} (Table 1). In comparison, the fidelity of tpol λ with the same single-nucleotide-gapped DNA is also sequence-dependent and in the range of 10^{-2} – 10^{-4} (15). Therefore, the full-length pol λ is 10- to 100-fold more faithful than the C-terminal fragment pol λ in filling single-nucleotide-gapped DNA. To ensure the fidelity difference between fpol λ and tpol λ was not due to experimental errors, we repeated the above fidelity and kinetic measure-

TABLE 1

Kinetic parameters of nucleotide incorporation into single-nucleotide-gapped DNA catalyzed by the full-length pol λ at 37 °C

dNTP	K_d	k_p	k_p/K_d	Fidelity ^a	Efficiency
	μM	s^{-1}	$\text{M}^{-1}\text{s}^{-1}$		Ratio ^b
Template A (D-1)					
dTTP	2.6 ± 0.4	3.9 ± 0.2	1.5×10^6	1	1.9
dATP	1.86 ± 0.09	0.00034 ± 0.00001	1.8×10^1	1.2×10^{-5}	16
dCTP	10.4 ± 0.3	0.0052 ± 0.0009	5.0×10^2	3.3×10^{-4}	22
dGTP	3.2 ± 0.5	0.00040 ± 0.00002	1.3×10^2	8.7×10^{-5}	20
Template G (D-6)					
dCTP	0.9 ± 0.1	1.57 ± 0.04	1.8×10^6	1	1.5
dATP	3 ± 1	0.00010 ± 0.00004	3.3×10^1	1.8×10^{-5}	20
dTTP	2.5 ± 0.3	0.00070 ± 0.00001	2.8×10^2	1.6×10^{-4}	23
dGTP	4 ± 1	0.00020 ± 0.00001	5.0×10^1	2.8×10^{-5}	13
Template T (D-7)					
dATP	0.9 ± 0.3	1.5 ± 0.1	1.6×10^6	1	1.4
dTTP	8.4 ± 0.6	0.0002 ± 0.0001	2.4×10^1	1.5×10^{-5}	88
dCTP	5.4 ± 0.2	0.004 ± 0.002	7.0×10^2	4.4×10^{-4}	11
dGTP	7 ± 4	0.010 ± 0.002	1.4×10^3	8.8×10^{-4}	51
Template C (D-8)					
dGTP	2.1 ± 0.3	2.5 ± 0.1	1.2×10^6	1	1.8
dATP	1.5 ± 1.0	0.0003 ± 0.0003	1.7×10^2	1.4×10^{-4}	19
dCTP	4.7 ± 0.3	0.002 ± 0.002	3.8×10^2	3.2×10^{-4}	17
dTTP	3.4 ± 0.1	0.00047 ± 0.00001	1.4×10^2	1.2×10^{-4}	10

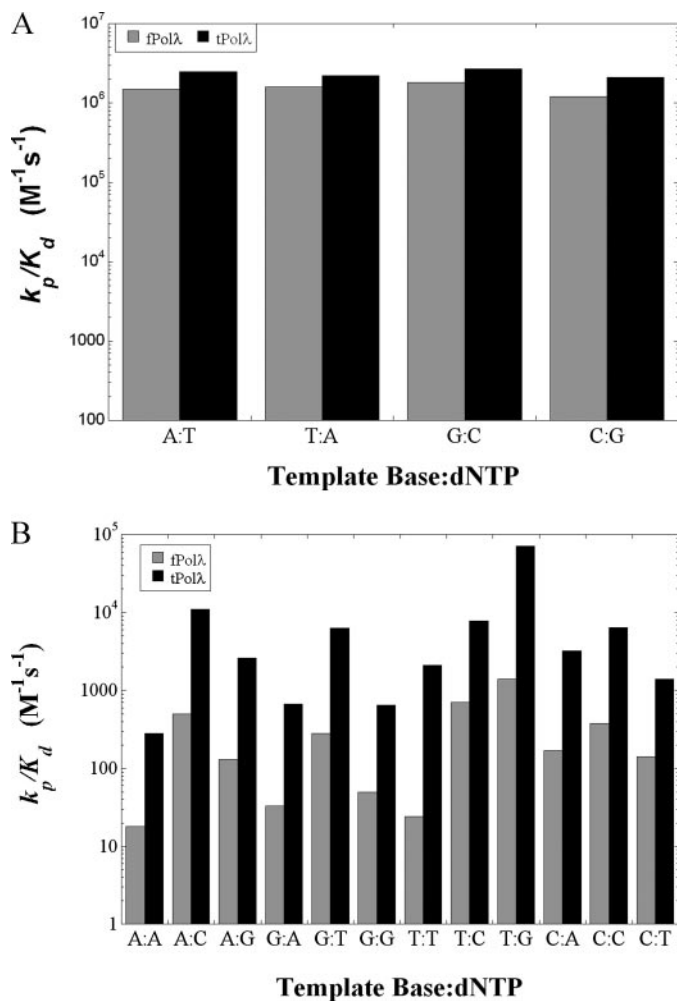
^a Calculated as $(k_p/K_d)_{\text{incorrect}} / [(k_p/K_d)_{\text{correct}} + (k_p/K_d)_{\text{incorrect}}]$.^b Calculated as $(k_p/K_d)_{\text{tpol}\lambda} / (k_p/K_d)_{\text{fpol}\lambda}$. The k_p/K_d values for tpol λ are from Table 2 of Ref. 15.

FIGURE 4. Comparison of the substrate specificity (k_p/K_d) for nucleotide incorporation catalyzed by fpol λ (Table 1) and tpol λ (15) separately. A, four correct incorporations; B, twelve incorrect incorporations. The y-axis is in the log scale.

ments with both fpol λ and tpol λ individually and obtained almost identical fidelity values (data not shown) to those corresponding values listed in Table 1 from our previously publication (15). The significant increase in fidelity from tpol λ to fpol λ is probably due to the presence of the BRCT domain, the proline-rich domain, or both.

Fidelity of dpol λ —To identify which of the one or more N-terminal domains up-regulates the fidelity of the full-length pol λ , we engineered and purified a fragment, dpol λ (residues 132–575, Fig. 1), that lacks the BRCT domain. With two diagnostic substrates D-6 and D-7, the kinetic parameters and fidelity of dpol λ were determined in the same manner as described above and are listed in Table 2. dpol λ incorporated nucleotides into D-6 and D-7 with a fidelity in the range of 10^{-4} – 10^{-5} , which was very similar to the fidelity of fpol λ (Table 1). The nucleotide incorporation efficiency ratios, $(k_p/K_d)_{\text{dpol}\lambda} / (k_p/K_d)_{\text{fpol}\lambda}$, were calculated to be in the range of 0.5–2.1 (Table 2 and Fig. 5). The average ratio for all eight possible nucleotide incorporations into both D-6 and D-7 was calculated to be 1.2. These ratios indicate that the substrate specificity of nucleotides with dpol λ , $(k_p/K_d)_{\text{dpol}\lambda}$, whether slightly larger or smaller, was within 2-fold of the substrate specificity of corresponding nucleotides with fpol λ , $(k_p/K_d)_{\text{fpol}\lambda}$. Because 2-fold differences are considered kinetically insignificant (20), we concluded that dpol λ and fpol λ have very similar, if not identical, gap-filling efficiency. Thus, the deletion of the BRCT domain in dpol λ did not affect the nucleotide incorporation efficiency and the fidelity of fpol λ . Similar polymerization efficiency and fidelity of dpol λ and fpol λ also indirectly confirmed that the N-terminal hexahistidine tag only present in the recombinant fpol λ did not affect the fidelity of fpol λ . Comparison of the fidelity of fpol λ (10^{-4} – 10^{-5} , Table 1), dpol λ (10^{-4} – 10^{-5} , Table 2), and tpol λ (10^{-2} – 10^{-4}) (15) reveals an intriguing conclusion: the non-enzymatic proline-rich domain alone significantly enhanced the fidelity of human pol λ .

TABLE 2

Kinetic parameters of nucleotide incorporation into single-nucleotide-gapped D-6 and D-7 catalyzed by dpol λ at 37 °C

dNTP	K_d	k_p	k_p/K_d	Fidelity ^a	Efficiency
	μM	s^{-1}	$\text{M}^{-1} \text{s}^{-1}$		Ratio ^b
Template G (D-6)					
dCTP	1.1 \pm 0.1	1.7 \pm 0.2	1.6 $\times 10^6$	1	0.89
dATP	3.2 \pm 0.9	0.00010 \pm 0.00002	3.3 $\times 10^1$	2.1 $\times 10^{-5}$	1.0
dTTP	1.8 \pm 0.8	0.00030 \pm 0.00007	1.7 $\times 10^2$	1.1 $\times 10^{-4}$	0.61
dGTP	3.3 \pm 0.5	0.00022 \pm 0.00002	6.7 $\times 10^1$	4.2 $\times 10^{-5}$	1.3
Template T (D-7)					
dATP	1.0 \pm 0.4	1.8 \pm 0.2	1.8 $\times 10^6$	1	1.1
dTTP	11 \pm 6	0.00046 \pm 0.00005	4.2 $\times 10^1$	2.3 $\times 10^{-5}$	1.7
dCTP	4 \pm 2	0.006 \pm 0.001	1.5 $\times 10^3$	8.3 $\times 10^{-4}$	2.1
dGTP	5 \pm 1	0.0087 \pm 0.0001	1.7 $\times 10^3$	9.4 $\times 10^{-4}$	1.2

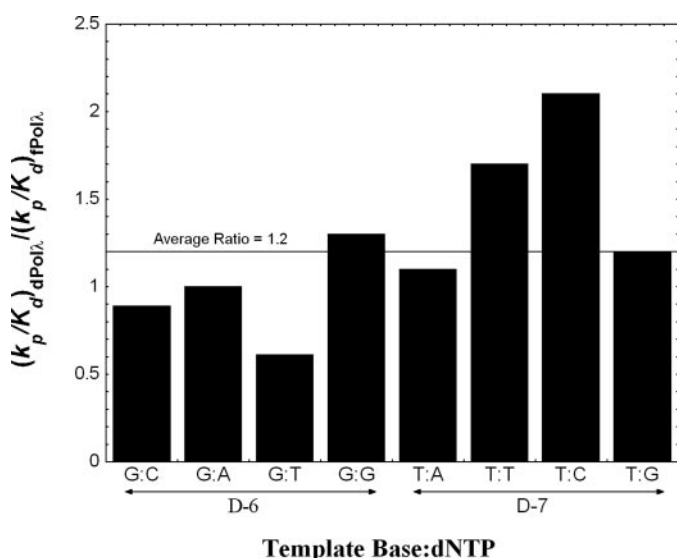
^a Calculated as $(k_p/K_d)_{\text{incorrect}} / [(k_p/K_d)_{\text{correct}} + (k_p/K_d)_{\text{incorrect}}]$.^b Calculated as $(k_p/K_d)_{\text{dpol}\lambda} / (k_p/K_d)_{\text{fpol}\lambda}$.

FIGURE 5. Both dpol λ (Table 2) and fpol λ (Table 1) incorporate nucleotides with similar efficiency with an average ratio of $(k_p/K_d)_{\text{dpol}\lambda} / (k_p/K_d)_{\text{fpol}\lambda}$ (Table 2) equal to 1.2 (indicated by the line) for all nucleotide incorporations into D-6 and D-7.

DISCUSSION

DNA polymerases λ and β share high sequence homology (54%) and sequence identity (33%) (1–3, 8). pol λ , like pol β , possesses the two key enzymatic activities (gap-filling polymerase and deoxyribose-5-phosphate lyase) required by BER. The role of pol λ in DNA repair is further supported by the following observations: (i) like pol β (21), pol λ is expressed at high levels in the developing mouse testes, suggesting a possible function of pol λ in DNA repair pathways associated with meiotic recombination (1); (ii) in an *in vitro* BER reconstitution assay, recombinant human pol λ and pol β can replace each other to efficiently repair uracil-containing DNA in the presence of human uracil-DNA glycosylase, human AP endonuclease, and human DNA ligase I (22); (iii) pol λ is the only X-family DNA polymerase found in higher plants and is induced by DNA-damaging treatments (23); (iv) mouse embryonic fibroblast cell extract contains substantial amounts of active pol λ , which contributes to uracil-initiated short-patch BER (16); (v) monoclonal antibodies against pol λ strongly reduce *in vitro* BER in the pol $\beta^{-/-}$ cell extract (16); and (vi) pol λ protects mouse fibroblasts against oxidative DNA damage and is recruited to oxidative DNA damage sites (24). Thus, pol λ may complement or support the func-

tion of pol β in BER *in vivo*. But this hypothesized role was initially weakened by the observed difference in single-nucleotide gap-filling fidelity between pol β and tpol λ . The fidelity of tpol λ (10^{-2} – 10^{-4}) (15) is ~ 10 - to 100-fold lower than the fidelity of rat pol β (recalculated as 10^{-4} – 10^{-5} using the definition of fidelity in Table 1), which was measured under similar single-turnover conditions with four single-nucleotide-gapped DNA 25–19/45-mer (primer-primer/template) substrates (25). If the full-length pol λ had similar fidelity to tpol λ , it would make 10- to 100-fold more base substitution errors than pol β if it participated in the repair of single-base lesions. DNA base modifications/losses are known to account for a large portion of total cellular DNA damage.

Under single-turnover conditions, the deoxyribonucleotide incorporation fidelity of human fpol λ was measured in the presence of four different single-nucleotide-gapped DNA substrates shown in Fig. 2. Surprisingly, the fidelity of fpol λ was determined to be in the range of 10^{-4} – 10^{-5} (Table 1) and was indeed significantly higher than that of tpol λ (10^{-2} – 10^{-4}) (15). This range for fpol λ was identical to the fidelity range determined for pol β (26). In addition, the efficiency for correct nucleotide incorporation into single-nucleotide-gapped DNA catalyzed by fpol λ (1.2×10^6 – $1.8 \times 10^6 \text{ M}^{-1} \text{ s}^{-1}$, Table 1) was only slightly lower than pol β (4×10^6 – $6 \times 10^6 \text{ M}^{-1} \text{ s}^{-1}$) (26). Similar polymerization efficiency and fidelity in combination with other biological evidence discussed above strongly support the hypothesis that pol λ and pol β both possess similar *in vivo* roles, such as functioning in BER. So far, the generation of knock-out mice through deletion of exons 5–7 of the pol λ gene has not yet confirmed the involvement of pol λ in BER or any other biological processes (27). The published mouse pol λ knock-out experiments (27, 28) are likely complicated by the existence of pol β (28), which could fill in and compensate for the loss of functional pol λ .

The measured fidelity of fpol λ (Table 1) was 10- to 100-fold higher than the fidelity of tpol λ (10^{-2} to 10^{-4}), estimated by employing the same single-turnover kinetic assay with identical DNA substrates (15). This indicated that the N-terminal domains of pol λ (Fig. 1) significantly enhance the fidelity of pol λ . Because tpol λ possesses slightly higher correct nucleotide incorporation efficiency than fpol λ (Table 1) and both enzymes bind to all correct and incorrect nucleotides with similarly high affinity (Table 1 and Ref. 15), it is unlikely that the absence of the N-terminal domains will cause any type of misfolding of

tpol λ and thus contribute to its low fidelity. This assumption was validated based on the following structural evidence: (i) when the high resolution tpol λ binary structure (2.1 Å) (12) and the full-length pol β ternary structure (2.2 Å) (14) are overlaid, the α carbons superimposed very well with a root mean square deviation of 1.4 Å for 113 C- α atoms (12), suggesting that tpol λ folds well and similarly to pol β in the absence of the two N-terminal domains of pol λ and (ii) no unfolded regions in tpol λ are observed in its 1.95–2.3 Å binary (12) and ternary crystal structures (11). Interestingly, the average ratio of $(k_p/K_d)_{\text{dpol}\lambda}/(k_p/K_d)_{\text{fpol}\lambda}$ for all eight possible nucleotide incorporation with D-6 and D-7 was 1.2 (Fig. 5), indicating that dpol λ and fpol λ almost have equal nucleotide incorporation efficiency. As expected, these two enzymes also have very similar fidelity (Tables 1 and 2). Thus, the deletion of the BRCT domain affected neither the single-nucleotide gap-filling efficiency nor the fidelity of pol λ , whereas differences in fidelity between dpol λ and tpol λ demonstrated that the non-enzymatic proline-rich domain dramatically enhanced the fidelity of pol λ by up to a 100-fold. This conclusion is consistent with the proposed function of the BRCT domain, which is generally known to mediate the protein-protein or protein-DNA interactions required for particular DNA repair pathways and cellular responsiveness to DNA damage (1–3, 8). Our conclusion is also supported by the observation of Shimazaki *et al.* (6) in which they found that deletion of the BRCT domain of human pol λ did not affect DNA synthesis with DNA substrates, including poly(dA)/oligo(dT) and activated DNA. The proline-rich domain has been proposed to merely couple polymerase action to the protein-protein and protein-DNA interactions required during DNA repair (1). Thus, the proline-rich domain is generally assumed to be dispensable for the polymerase activity of pol λ . However, the difference in fidelity between tpol λ and dpol λ observed here suggested that the flexible proline-rich domain actively regulates the polymerase fidelity. Enhancement of the fidelity of a polymerase by a non-enzymatic domain is both surprising and unprecedented. Therefore, the 11-kDa proline-rich domain must interact with the subdomains of tpol λ and optimize the geometry of the polymerase active site to achieve higher fidelity. The fidelity modulation observed here differs dramatically from the fidelity enhancement contributed by the enzymatic activity of a 3'→5' exonuclease domain of a replicative DNA polymerase, or by an accessory protein as in the case of the mitochondrial DNA polymerase complex (29). Amazingly, the enhancement of the pol λ fidelity by the proline-rich domain is as large as what has been contributed by the proofreading 3'→5' exonuclease domain to a replicative DNA polymerase (29, 30). Our results further suggest that DNA polymerases, the vital enzymes that replicate and maintain genomic DNA, have evolved through different mechanisms to adjust their polymerization fidelity to best perform diverse physiological functions.

Interestingly, the fidelity difference between tpol λ and fpol λ resulted mainly from stronger discrimination against mismatched nucleotides by fpol λ . The average substrate specificity of misincorporations was 10- to 100-fold lower with fpol λ than with tpol λ (Fig. 4B). In comparison, fpol λ incorporated correct dNTPs with an efficiency (k_p/K_d) of $(1.2\text{--}1.8) \times 10^6 \text{ M}^{-1}\text{s}^{-1}$ (Table 1), which was only ~2-fold lower than the correspond-

Fidelity of DNA pol λ Measured by Transient Kinetics

ing range of $(2.1\text{--}2.7) \times 10^6 \text{ M}^{-1}\text{s}^{-1}$ with tpol λ (Fig. 4A). The larger decrease in the incorporation efficiency of mismatched over matched dNTPs (Table 1 and Fig. 4) with fpol λ led to the higher fidelity of pol λ . In comparison, the accessory subunit enhances the fidelity of mitochondrial DNA polymerase by 14-fold by increasing the incorporation efficiency of a correct A:T base pair more than a T:T mismatch (29). Furthermore, the decrease in the incorporation efficiency of both matched and mismatched dNTPs was due to slower incorporation rate constants (k_p) with fpol λ than with tpol λ , because the binding of all dNTPs (K_d) by these two enzymes was similarly tight (Table 1 and Ref. 15). This suggested fpol λ was slower yet more faithful than tpol λ in filling single-nucleotide-gapped DNA. This correlation goes against the general trend summarized from a survey of the A-, B-, X-, and Y-families by Beard *et al.* (31) that a more catalytically efficient polymerase has a lower base substitution rate. It is not clear what contributes to this intriguing correlation between the polymerase fidelity and nucleotide incorporation rate. We speculate that the presence of the proline-rich domain in both fpol λ and dpol λ may either somewhat tighten the polymerase active site to achieve better geometric selection (32, 33), or shield the active site of pol λ from solvent, which leads to greater desolvation of a nascent base pair and amplifies the free energy differences between matched and mismatched nucleotide incorporations (34). These possibilities can be evaluated by the active site structural differences between the ternary crystal structures of fpol λ (or dpol λ)·single-nucleotide-gapped DNA·dNTP and tpol λ ·single-nucleotide-gapped DNA·dNTP (11), especially in the presence of a mismatched incoming nucleotide.

REFERENCES

- Garcia-Diaz, M., Dominguez, O., Lopez-Fernandez, L. A., de Lera, L. T., Saniger, M. L., Ruiz, J. F., Parraga, M., Garcia-Ortiz, M. J., Kirchhoff, T., del Mazo, J., Bernad, A., and Blanco, L. (2000) *J. Mol. Biol.* **301**, 851–867
- Aoufouchi, S., Flatter, E., Dahan, A., Faili, A., Bertocci, B., Storck, S., Delbos, F., Cocea, L., Gupta, N., Weill, J. C., and Reynaud, C. A. (2000) *Nucleic Acids Res.* **28**, 3684–3693
- Nagasawa, K., Kitamura, K., Yasui, A., Nimura, Y., Ikeda, K., Hirai, M., Matsukage, A., and Nakanishi, M. (2000) *J. Biol. Chem.* **275**, 31233–31238
- Filee, J., Forterre, P., Sen-Lin, T., and Laurent, J. (2002) *J. Mol. Evol.* **54**, 763–773
- Bork, P., Hofmann, K., Bucher, P., Neuwald, A. F., Altschul, S. F., and Koonin, E. V. (1997) *FASEB J.* **11**, 68–76
- Shimazaki, N., Yoshida, K., Kobayashi, T., Toji, S., Tamai, K., and Koivai, O. (2002) *Genes Cells* **7**, 639–651
- Fan, W., and Wu, X. (2004) *Biochem. Biophys. Res. Commun.* **323**, 1328–1333
- Garcia-Diaz, M., Bebenek, K., Sabariego, R., Dominguez, O., Rodriguez, J., Kirchhoff, T., Garcia-Palomero, E., Picher, A. J., Juarez, R., Ruiz, J. F., Kunkel, T. A., and Blanco, L. (2002) *J. Biol. Chem.* **277**, 13184–13191
- Sobol, R. W., Horton, J. K., Kuhn, R., Gu, H., Singhal, R. K., Prasad, R., Rajewsky, K., and Wilson, S. H. (1996) *Nature* **379**, 183–186
- Singhal, R. K., Prasad, R., and Wilson, S. H. (1995) *J. Biol. Chem.* **270**, 949–957
- Garcia-Diaz, M., Bebenek, K., Krahn, J. M., Kunkel, T. A., and Pedersen, L. C. (2005) *Nat. Struct. Mol. Biol.* **12**, 97–98
- Garcia-Diaz, M., Bebenek, K., Krahn, J. M., Blanco, L., Kunkel, T. A., and Pedersen, L. C. (2004) *Mol. Cell* **13**, 561–572
- Pelletier, H., Sawaya, M. R., Kumar, A., Wilson, S. H., and Kraut, J. (1994) *Science* **264**, 1891–1903
- Sawaya, M. R., Prasad, R., Wilson, S. H., Kraut, J., and Pelletier, H. (1997) *Biochemistry* **36**, 11205–11215

Fidelity of DNA pol λ Measured by Transient Kinetics

15. Fiala, K. A., Abdel-Gawad, W., and Suo, Z. (2004) *Biochemistry* **43**, 6751–6762
16. Braithwaite, E. K., Prasad, R., Shock, D. D., Hou, E. W., Beard, W. A., and Wilson, S. H. (2005) *J. Biol. Chem.* **280**, 18469–18475
17. Ramadan, K., Shevelev, I. V., Maga, G., and Hubscher, U. (2002) *J. Biol. Chem.* **277**, 18454–18458
18. Bebenek, K., Garcia-Diaz, M., Blanco, L., and Kunkel, T. A. (2003) *J. Biol. Chem.* **278**, 34685–34690
19. Lee, J. W., Blanco, L., Zhou, T., Garcia-Diaz, M., Bebenek, K., Kunkel, T. A., Wang, Z., and Povirk, L. F. (2004) *J. Biol. Chem.* **279**, 805–811
20. Johnson, K. A. (1992) *The Enzymes* **20**, 1–61
21. Hirose, F., Hotta, Y., Yamaguchi, M., and Matsukage, A. (1989) *Exp. Cell Res.* **181**, 169–180
22. Garcia-Diaz, M., Bebenek, K., Kunkel, T. A., and Blanco, L. (2001) *J. Biol. Chem.* **276**, 34659–34663
23. Uchiyama, Y., Kimura, S., Yamamoto, T., Ishibashi, T., and Sakaguchi, K. (2004) *Eur. J. Biochem.* **271**, 2799–2807
24. Braithwaite, E. K., Kedar, P. S., Lan, L., polosina, Y. Y., Asagoshi, K., poltoratsky, V. P., Horton, J. K., Miller, H., Teebor, G. W., Yasui, A., and Wilson, S. H. (2005) *J. Biol. Chem.* **280**, 31641–31647
25. Ahn, J., Kraynov, V. S., Zhong, X., Werneburg, B. G., and Tsai, M. D. (1998) *Biochem. J.* **331**, 79–87
26. Ahn, J., Werneburg, B. G., and Tsai, M. D. (1997) *Biochemistry* **36**, 1100–1107
27. Bertocci, B., De Smet, A., Flatter, E., Dahan, A., Bories, J. C., Landreau, C., Weill, J. C., and Reynaud, C. A. (2002) *J. Immunol.* **168**, 3702–3706
28. Kobayashi, Y., Watanabe, M., Okada, Y., Sawa, H., Takai, H., Nakanishi, M., Kawase, Y., Suzuki, H., Nagashima, K., Ikeda, K., and Motoyama, N. (2002) *Mol. Cell Biol.* **22**, 2769–2776
29. Johnson, A. A., and Johnson, K. A. (2001) *J. Biol. Chem.* **276**, 38090–38096
30. Johnson, A. A., and Johnson, K. A. (2001) *J. Biol. Chem.* **276**, 38097–38107
31. Beard, W. A., Shock, D. D., Vande Berg, B. J., and Wilson, S. H. (2002) *J. Biol. Chem.* **277**, 47393–47398
32. Kool, E. T. (2002) *Annu. Rev. Biochem.* **71**, 191–219
33. Goodman, M. F. (1997) *Proc. Natl. Acad. Sci. U. S. A.* **94**, 10493–10495
34. Petruska, J., Sowers, L. C., and Goodman, M. F. (1986) *Proc. Natl. Acad. Sci. U. S. A.* **83**, 1559–1562